

Chameleon: Virtualizing Idle Acceleration Cores of A Heterogeneous Multicore Processor for Caching and Prefetching

DONG HYUK WOO

Georgia Institute of Technology

JOSHUA B. FRYMAN and ALLAN D. KNIES

Intel Corporation

and

HSIEN-HSIN S. LEE

Georgia Institute of Technology

3

Heterogeneous multicore processors have emerged as an energy- and area-efficient architectural solution to improving performance for domain-specific applications such as those with a plethora of data-level parallelism. These processors typically contain a large number of small, compute-centric cores for acceleration while keeping one or two high-performance ILP cores on the die to guarantee single-thread performance. Although a major portion of the transistors are occupied by the acceleration cores, these resources will sit idle when running unparallelized legacy codes or the sequential part of an application. To address this underutilization issue, in this article, we introduce Chameleon, a flexible heterogeneous multicore architecture to virtualize these resources for enhancing memory performance when running sequential programs. The Chameleon architecture can dynamically virtualize the idle acceleration cores into a last-level cache, a data prefetcher, or a hybrid between these two techniques. In addition, Chameleon can operate in an adaptive mode that dynamically configures the acceleration cores between the hybrid mode and the prefetch-only mode by monitoring the effectiveness of the Chameleon cache mode. In our evaluation with SPEC2006 benchmark suite, different levels of performance improvements were achieved in different modes for different applications. In the case of the adaptive mode, Chameleon improves the performance of SPECint06 and SPECfp06 by 31% and 15%, on average. When considering only memory-intensive applications, Chameleon improves the system performance by 50% and 26% for SPECint06 and SPECfp06, respectively.

This research was supported by an NSF grant CCF-0811738, an NSF CAREER award CNS-0644096, and gift from Intel Corporation.

Authors' addresses: D. H. Woo, Georgia Institute of Technology; J. B. Fryman and A. D. Knies, Intel Corporation; H.-H. S. Lee, Georgia Institute of Technology.

Permission to make digital or hard copies of part or all of this work for personal or classroom use is granted without fee provided that copies are not made or distributed for profit or commercial advantage and that copies show this notice on the first page or initial screen of a display along with the full citation. Copyrights for components of this work owned by others than ACM must be honored. Abstracting with credit is permitted. To copy otherwise, to republish, to post on servers, to redistribute to lists, or to use any component of this work in other works requires prior specific permission and/or a fee. Permissions may be requested from Publications Dept., ACM, Inc., 2 Penn Plaza, Suite 701, New York, NY 10121-0701 USA, fax +1 (212) 869-0481, or permissions@acm.org.
© 2010 ACM 1544-3566/2010/04-ART3 \$5.00
DOI 10.1145/1736065.1736068 <http://doi.acm.org/10.1145/1736065.1736068>

ACM Transactions on Architecture and Code Optimization, Vol. 7, No. 1, Article 3, Publication date: April 2010.

Categories and Subject Descriptors: B.3.2 [**Memory Structures**]: Design Styles—*Cache memories*; C.1.2 [**Processor Architectures**]: Multiple Data Stream Architectures (Multiprocessors)—*Array and vector processors*

General Terms: Design, Experimentation, Performance

Additional Key Words and Phrases: Heterogeneous multicore, idle core, cache, prefetching

ACM Refranch Format:

Woo, D. H., Fryman, J. B., Knies, A. D., Lee, H.-H. S. 2010. Chameleon: Virtualizing idle acceleration cores of a heterogeneous multicore processor for caching and prefetching. *ACM Trans. Architect. Code Optim.* 7, 1, Article 3 (April 2010), 35 pages.

DOI = 10.1145/1736065.1736068 <http://doi.acm.org/10.1145/1736065.1736068>

1. INTRODUCTION

Heterogeneous computing has emerged to address the growing concerns of energy efficiency [Woo and Lee 2008] and silicon area effectiveness [Hill and Marty 2008]. Small-scale heterogeneous MPSoCs have been used in embedded systems for years [Dutta et al. 2001; Artieri 2005]. Meanwhile, general-purpose processor designers are also advocating such heterogeneous architectures for future multicore or many-core processors to optimize a system's energy efficiency (measured in performance per joule) or area effectiveness (measured in performance per mm²). For example, the first generation of the IBM Cell Broadband Engine (Cell/BE) [Pham et al. 2005] integrated eight synergistic processing elements along with a superscalar PowerPC processor on the same die. CUDA [Buck 2007], CTM [Hensley 2007], RapidMind [McCool et al. 2006], OpenCL [Munshi 2008], PeakStream [Papakipos 2006], and Ct [Ghuloum et al. 2007] abstract the programming interface to enable heterogeneous computing based on a cooperative computing model between the CPU(s) and many-core graphics processing units (GPUs), shielding programmers from managing the complexity of these heterogeneous components. Although some heterogeneous computing platforms have their resources distributed across multiple chips, the trend of future technology is toward integrating them all onto the same die [Moore 2007].

Unlike a symmetric multicore processor in which all processor cores are identical, a heterogeneous computing platform is composed of distinct classes of processing cores: a high-performance host processor and an array of acceleration processing elements (PEs) [Pham et al. 2005; Moore 2007; Smith 2008; Woo et al. 2008; Singh et al. 2000; Yeh et al. 2007; Mahesri et al. 2008]. The high-performance host processor is mainly used for exploiting the sequential performance of an application. In contrast, the acceleration PE cores, typically not designed with complex ILP techniques, are integrated to deliver high throughput for parallelizable code with better energy and area efficiency. The rationale behind such a heterogeneous multicore design is (i) to improve the energy efficiency and manage its ensuing thermal issues when running data-parallel workloads and (ii) not to lose sequential performance.

Unfortunately, while the host processor executes the sequential code of a parallelized workload or unparallelized legacy applications, the acceleration cores of a heterogeneous multicore processor become idle, contributing nothing

to single-thread performance while consuming area and additional power if not completely turned off. From the standpoints of area and energy efficiency, the unused idle resources could dwarf the interests of adopting such a heterogeneous platform for general-purpose computing. To address this underutilization problem during sequential computation, we envision that we could better utilize these idle PE resources to accelerate the sequential execution on the host processor. In this article, we introduce *Chameleon*, a flexible architecture with low-cost enabling techniques to provide several dynamic operation modes for better resource allocation. In addition to the parallel acceleration mode, the PE cores in Chameleon can be configured into a last-level cache, a data prefetcher, and variants of their combinations when running sequential programs. The main contributions of this work are as follows.

- We propose the Chameleon heterogeneous multicore architecture, which virtualizes otherwise unused acceleration cores to enable prefetching and additional cache space when running sequential workloads. We also show that the extra hardware cost to realize Chameleon is not significant.
- We propose several different operation modes including a caching mode, a data prefetching mode, and a hybrid mode to virtualize the acceleration cores collectively for enhancing memory performance. In addition, we also propose an adaptive mode to change these modes dynamically to adapt the memory behavior of applications.
- We perform a case study using a heterogeneous multicore processor that consists of a host processor integrated with an on-die massively parallel SIMD accelerator. We justify the performance benefits given by Chameleon and evaluate the hardware/power overheads and energy implications.

This article is organized as follows: Section 2 explains the architectural features of our baseline heterogeneous multicore processor. Section 3 enumerates different design issues for providing a virtualized last-level cache and a virtualized prefetcher. It also describes the hybrid and the adaptive designs. Section 4 evaluates the characteristics of these different design choices and demonstrates single-thread performance improvement of SPEC 2006 benchmark suite. Section 5 discusses other issues of Chameleon's implementation, and Section 6 enumerates related work. Finally, Section 7 concludes the article.

2. BASELINE MULTICORE ARCHITECTURE

Although the core concept of Chameleon, utilizing idle acceleration cores for improving the performance of sequential workloads, can be generally applied to many heterogeneous multicore processors, the detailed design as well as its benefit and associated hardware overheads will vary for different heterogeneous architectures. In this article, we investigated a Chameleon architecture based on a recently proposed accelerator architecture [Woo et al. 2008] and evaluated its cost and performance potentials. We will later briefly discuss how Chameleon can be applied to other architectures in Section 5.

Figure 1 illustrates our baseline heterogeneous multicore processor used throughout this article [Woo et al. 2008]. It consists of a state-of-the-art

PEs are connected to a Direct Memory Access (DMA) engine called *Row Response Queue (RRQ)*. An RRQ and all PEs in the same row are connected through a memory bus (MBus), which consists of two unidirectional buses. One bus streams data back from the main memory to the PEs in the row, and the other bus streams data from the PEs in the row to the main memory. PEs can also communicate with each other through a mesh network.¹ Communication is fully software controlled by a communication instruction, which allows each PE to transfer 64-bit or 128-bit data to one of its four neighbor PEs. Because all communication is fully controlled by explicit instructions and because all execution is fully orchestrated by the host processor, communication patterns are completely deterministic and exempt from issues caused by bus arbitration, congestion, deadlock, and live-lock. Furthermore, each PE only needs a single 4:1 mux and 1:4 demux for its mesh communication. Therefore, no area- and power-hungry router is required.

3. CHAMELEON ARCHITECTURE

Here, we describe our proposed architecture called *Chameleon* for future heterogeneous multicore processors. To achieve better utilization of on-die resources, we added low-cost configuration hardware that virtualizes idle acceleration cores dynamically to improve sequential performance. With Chameleon techniques, idle cores can be virtualized into (i) a unified last-level cache, (ii) a data prefetcher, or (iii) a hybrid caching/prefetching component. In addition, we propose an adaptive operation mode that changes Chameleon among different modes to find the best possible performance by exploiting the dynamic behavior of an application.

3.1 C-Mode: Virtualizing Idle Cores for Caching

As shown in Section 2, the original purpose of integrating a heterogeneous PE array onto general-purpose processor cores is to exploit Data-Level Parallelism (DLP) for maximizing energy and area efficiency. We call this operation mode *A-mode* (or acceleration mode) to differentiate it from the new modes we will introduce. Our first goal is to virtualize this idled heterogeneous PE array into additional caching space when the A-mode is not in use. This virtualization must be simple and should not affect the efficiency of the A-mode. The idea is to configure the unused local scratchpad memories collectively into a last-level cache by using PEs' basic operations for caching control. We call this operation mode the *C-mode* (or caching mode). Similar to the A-mode, the PEs will be responsible for decoding instructions received from the IBus, performing corresponding local computation, and routing computation results back. For example, to calculate the cache index bits, the PE is programmed to perform an SHR (logical shift-right) to eliminate the cache line offset and an AND (logical and) to mask out tag bits. Using this calculated index bits, the PE can read data from its local 128KB scratchpad memory with a load instruction.

¹The mesh network can be reconfigured to a folded torus network using simple switches [Dally and Towles 2001; Siegel et al. 1984].

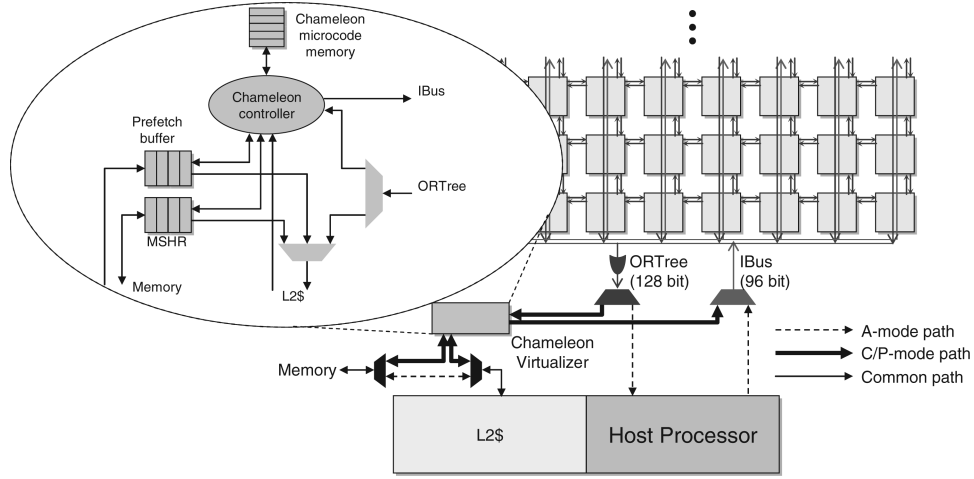


Fig. 2. Chameleon Virtualizer (not drawn to scale).

To control the PEs array and to have it function like a soft cache, we add a new interface between the L2 cache of the host processor and the baseline PE array. As shown in Figure 2, this new interface, called *Chameleon Virtualizer*, is in charge of orchestrating memory management operations for implementing the virtualized last-level cache using microcode stored inside the Chameleon microcode memory. The microcode is written in the original PE ISA, and it consists of tens of PE instructions. Upon a cache read miss in the L2 cache, for example, the miss address is forwarded to the Chameleon controller. Once receiving the address, the Chameleon controller forwards the miss address to the PEs via IBus and starts to broadcast a cache read microcode to the PEs. To perform a cache read, PEs perform the following tasks: (i) calculating cache index bits, (ii) matching valid and tag bits, and (iii) sending a hit/miss signal to the Chameleon Virtualizer. Upon a cache hit, the hit PE has to perform the following additional tasks: (iv) loading the cache line from the scratchpad memory, (v) routing the line back to the Chameleon Virtualizer, and (vi) updating the corresponding L2 LRU bits. Once the cache line reaches the Chameleon Virtualizer, it is forwarded to the L2. On the other hand, upon a cache miss, the Chameleon controller initiates an off-chip memory request through the MSHR of the Chameleon Virtualizer. The Chameleon Virtualizer also contains a prefetch buffer to support the virtualized prefetcher to be detailed in Section 3.2. Note that the overhead of the Chameleon Virtualizer is only incurred in the C-mode because the controller will be bypassed when operating in the conventional A-mode.

To facilitate the mechanisms for a cache line that hits in the PEs, we reuse the existing 128-bit wide ORTree bus, which was originally designed for obtaining the flag status of the PE array but will be idle when operating in the C-mode. Hence, we hijack this bus to send hit/miss signals and transfer requested cache lines. However, to use the ORTree bus for such purposes, we need to add a new instruction called *xferortree* into the PE's ISA. This special

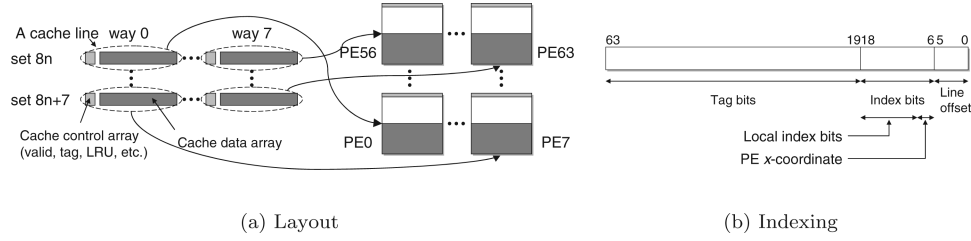


Fig. 3. Way-level parallelism (8-way cache, 4MB).

move instruction drives a register value onto the ORTree. This new instruction requires adding a mux in each PE for selecting either the flag status (in the A-mode) or the output operand of an `xferortree` instruction (in the C-mode) for ORTree. On the other hand, the Chameleon Virtualizer is connected to the other end of the ORTree. Note that, in our implementation, only one PE in the same column can transfer data to the Chameleon Virtualizer at any given time, and the ORTree output value of all other PEs in the column is zero. Thus, ORTree can safely deliver the data to the Chameleon Virtualizer without being corrupted by OR operations.

In the following sections, we will address the challenges with respect to the styles of cache line layout across the PE array. We also detail these design alternatives and evaluate and quantify their trade-offs in our experiments. Furthermore, we investigate how we can optimize their access latency by adopting nonuniform cache architecture (NUCA) and discuss the required architectural support.

3.1.1 Design for Way-Level Parallelism. Our first design is to distribute multiway cache lines of the same set across PEs in the same column. Figure 3 shows an example mapping of an 8-way set-associative 4MB cache. In this example, eight cache lines (each 64 bytes) mapped to the same cache set are distributed across eight PEs in the same column (e.g., PE0, PE8, to PE56). Also shown in the figure is how to index this cache. Out of the global index bits, three LSBs are used to find the x -coordinate of target PE column. The rest of the index bits (10 bits) are used as the local index for finding the cache line from the eight local scratchpad memories on the indexed column. (In this design, up to 1,024 cache lines can be stored inside each PE. This will be clarified later in this section.) Mask instructions are used to disable the other 56 PEs after the x -coordinate is calculated. In this particular design, all eight active PEs on the same column will perform a tag comparison in parallel. Hence, we say this design exploits Way-Level Parallelism (WLP).

One challenge for having a functional WLP cache is how to perform LRU updates across PEs in the same column. To solve this issue, we chose to implement the counter LRU algorithm [Kadota et al. 1987] and program Chameleon microcode to perform replacement operations. This software-based LRU replacement mechanism will read the LRU state of the hit line and broadcast the outcome back to all PEs in the same column. The PEs will then update their own LRU bits accordingly. Note that these updates simply use subtract and

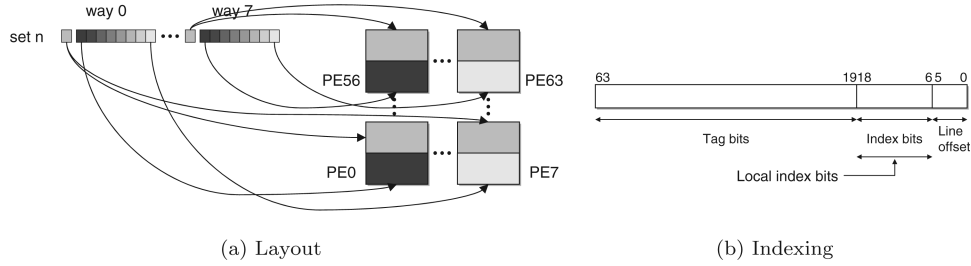


Fig. 4. Way- and subblock-level parallelism (8-way cache, 4MB).

compare instructions already provided by the PE ISA. Although a software-based LRU may take longer than a hardware-based LRU update, we found that that properly scheduled microcode can hide much of this latency.

On the other hand, this WLP design has a space overhead for cache control bits. To implement an 8-way 4MB cache with 64B line for a 64-bit host processor, we need one valid bit, one dirty bit, 45 tag bits, three LRU state bits, and a few coherence protocol bits for each cache line. These control bits amount to around 10% overhead. Thus, for N cache lines, the total storage needed will be $1.1 \times 64 \times N$ bytes, and it should fit into a 128KB scratchpad space. Furthermore, the number of sets stored in each PE should be a power of 2 for cache indexing. This explains why each PE accommodates 1,024 cache lines in our WLP design.

In this design, once the set is determined, only one corresponding column is enabled to complete one cache operation. In other words, if the Chameleon Virtualizer can provide eight instruction streams to different columns and decode eight returning messages, we can build a virtualized eight-bank cache. To implement it, eight different IBuses and eight different ORTree buses should be directly connected to the Chameleon Virtualizer instead of using fan-out tree (IBus) and fan-in OR tree (ORTree), as in the baseline processor.

3.1.2 Design for Way- and Subblock-Level Parallelism. Since the 128-bit ORTree bus and the 96-bit IBus are used for reading and writing cache lines in the WLP-style cache, it will take four and eight cycles to transfer an entire 64B cache line on the buses.² On the other hand, to prepare data transfer, four SIMD load instructions (or eight regular store instructions) are used to load each 16B chunk into the XMM registers (or store 8B chunk to general-purpose registers), which adds extra overheads in accessing cache lines. This is an artifact caused by mapping one entire cache line onto a single PE, as shown in Figure 3. To alleviate this issue, we investigate another design option in which a 64B cache line is split across eight PEs on the same row, as shown in Figure 4. To read a cache line in this design, each PE in the same row will load an 8B subblock of the requested cache line. All eight subblocks will be routed back to the Chameleon Virtualizer simultaneously without modifying the PE microarchitecture. We call this design exploiting Way- and subBlock-Level Parallelism (WBLP). Due to subblocking, we only need one load and one xferortree instruction for reading an entire cache line and one 64-bit immediate broadcast instruction and one store

²The 96-bit IBus can only broadcast 64-bit data at each cycle due to instruction-encoding overhead.

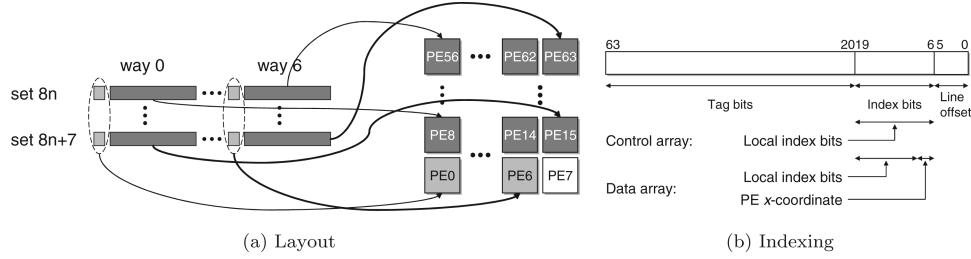


Fig. 5. Decoupled WLP cache (7-way cache, 7MB).

for writing it. In this design, the Chameleon Virtualizer is made to broadcast an immediate move operation with eight different immediate values and to retrieve eight different data return values. In this design, as in the eight-bank WLP-style cache, eight different IBuses and eight different ORTree buses should have direct connection to the Chameleon Virtualizer instead of using fan-out IBus and fan-in ORTree, as in the baseline processor.

The primary challenge of such a WBLP design is the area overhead in keeping the cache control bits. As a cache line is split into eight subblocks, all eight PEs that keep a subblock of the same cache line need to have redundant valid, tag, LRU, and coherence bits. Otherwise, more delay will incur for communicating this information. We found that each PE can accommodate this redundant information without sacrificing the overall cache capacity. As explained in Section 3.1.1, at most, 64-bit of overhead is required per 64B cache line. In the WLP design, out of the 128KB scratchpad memory per PE, 64KB is consumed by its data array, and less than 8KB is consumed by these cache control bits (i.e., each 128KB scratchpad memory is quite underutilized.) In the WBLP design, at most, 64-bit overhead is required per 8B subblock. Thus, 64KB is used by its data array, and at most 64KB is consumed by the cache control array with no further implication to utilizing the maximally available cache capacity.

3.1.3 Decoupled Design. The two designs discussed previously place the cache control array and data array in one PE so that each PE can locally detect whether the request is a hit or a miss and route the hit line back to the Chameleon Virtualizer. Such a local decision mechanism allows these two transfer operations to be pipelined so that the overall look-up latency can be reduced. However, as explained previously, these designs cannot utilize the memory space efficiently because the number of sets in each PE must be a power of 2.

Instead, we study an alternative design style where the cache control array and data array are spread across different PEs. In this design, the Chameleon Virtualizer needs to read the hit/miss signal first from PEs that store the cache control array, and then it needs to request the target PE that stores the hit line to route the line back to the Chameleon Virtualizer. Figures 5 and 6 show such decoupled designs. As shown in the figures, the cache control array is stored in seven PEs in row 0. The Chameleon Virtualizer needs to look up these PEs' local scratchpad memory space to see whether the requested block is a cache

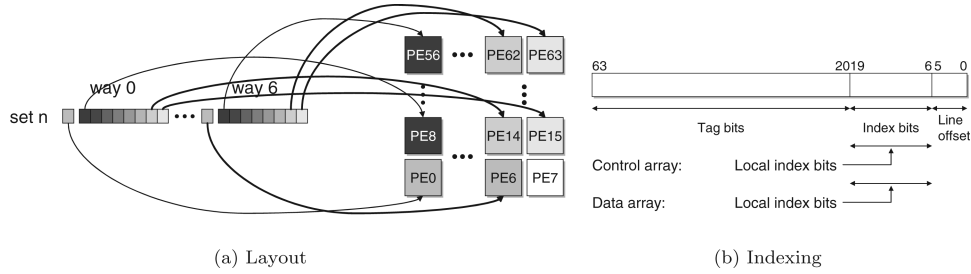


Fig. 6. Decoupled WBLP cache (7-way cache, 7MB).

hit or miss. Upon a hit, it also needs to request one (decoupled WLP) or eight (decoupled WBLP) PEs out of 56 PEs (row 1 to row 7) to route the hit data array back to the Chameleon Virtualizer. In our decoupled design, PE_n ($0 \leq n \leq 6$) keeps a cache control array for the data array of PEs in row $n + 1$. For example, in case of a decoupled WBLP cache (Figure 6), PE6 stores the cache control array of way 6, while the cache data array of way 6 is stored in PEs of row 7 (PE56 to PE63). Although the look-up latency of this style cache is longer than that of previous two designs, 7-way set-associative 7MB cache (total 16K sets) can be stored in 64 PEs—each of seven PEs in row 0 stores the cache control array of 16K cache lines of each way; each PE in other rows stores the cache data array of 2K lines (the decoupled WLP cache (Figure 5)) or the 8B subblock of 16k lines (the decoupled WBLP cache (Figure 6)). Note that these 63 PEs fully utilize their 128KB local scratchpad memory. The only unused space is the local memory space of PE7, as shown in the figures.

3.1.4 NUCA Cache Design. In the conventional A-mode, for synchronizing the computation for each PE, a PE located at row i (where i ranges from 0 to 7) in an 8×8 PE array contains an instruction queue with $7 - i$ entries as shown in Figure 7(a). Instructions are broadcast through IBus and queued prior to the execution by its designated PE. The delay units (shown as D blocks) are inserted to synchronize each instruction broadcast in a SIMD-style execution. With the instruction queue and pipelined IBus, PEs in different rows will execute the same instruction at the same cycle, fully synchronized. Similarly, a pipelined ORTree and flag queue are used to synchronize flag status globally. Such a strictly synchronized execution model keeps the architecture and its programming models simple. For example, neither the processor architects nor the programmers have to deal with complicated synchronization issues such as live-locks or deadlocks.

However, if the PEs are collectively used as a virtualized last-level cache, it will be beneficial to have nonuniform access latencies, that is, accessing each PE row out-of-sync. As shown in previous studies [Kim et al. 2002; Huh et al. 2005; Chishti et al. 2003], a non-uniform cache architecture (NUCA) helps reduce the average cache access latency, thereby improving the overall performance. As such, it will be more desirable to keep data with good temporal locality in a nearby memory bank of a large NUCA structure. Although our baseline PE array already has a partitioned array of 64 PEs that uses mesh

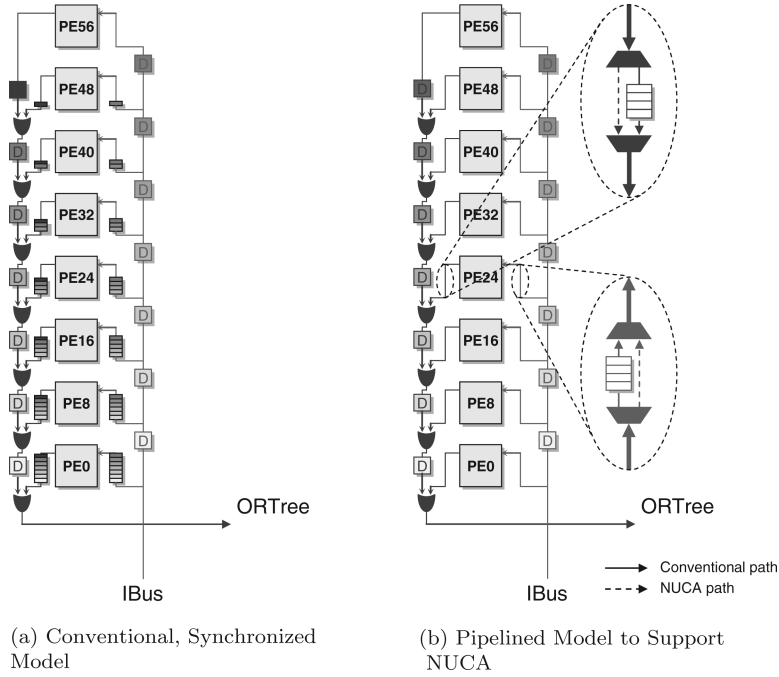


Fig. 7. Execution model (only column 0 is shown.).

topology, it requires certain changes in the architecture to enable nonuniform latencies across PE rows. To eliminate the strictly synchronized execution nature of the baseline, the instruction and flag queues, originally designed for synchronizing their broadcasting, are bypassed when the NUCA model is enabled. As shown in Figure 7(b), the NUCA path directly bypasses and does not buffer any incoming cache access microcode instruction and outgoing requested cache lines. Consequently, in this execution model, different PEs in different rows execute different instructions at the same cycle. However, the pipelined execution model could complicate the synchronization of the ORTree values and that of northbound and southbound transfer instructions. This is what we call *time-zone effect*. Fortunately, the ORTree time-zone effect is not an issue in the C-mode as C-mode microcode uses the ORTree to obtain a requested cache line. Furthermore, the Chameleon Virtualizer is allowed to issue one memory look-up microcode at a time, so no data is corrupted between distinct memory accesses. The northbound transfer instruction can be synchronized by adding one more pipeline register in the northbound output mesh driver, while the southbound transfer instruction can be synchronized by architecting the latency of this instruction as two cycles. More details on the time-zone effect can be found in Appendix A.

Another NUCA design issue is with respect to how to implement the LRU policy efficiently. Figure 8 illustrates an instance for our decoupled WLP cache. In this example, the host processor issues to read line 2, and seven PEs have seven different cache lines mapped to the same set, as shown in Figure 8(a). Upon

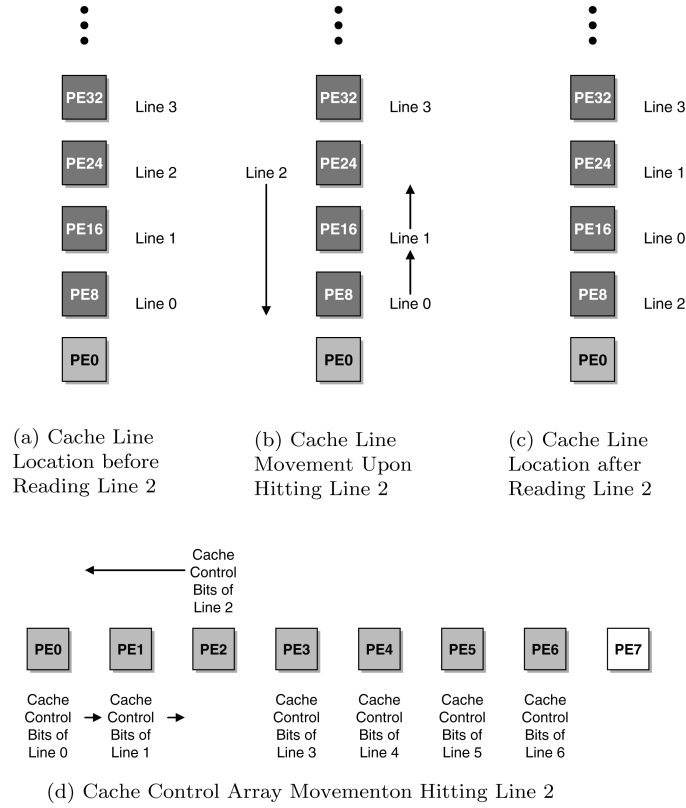


Fig. 8. LRU management of a NUCA C-mode (decoupled WLP cache).

detecting the requested line 2 in PE24, PE24 transfers it to the Chameleon Virtualizer, and those PEs whose row numbers are smaller than PE24 will transfer their cache lines to the north (Figure 8(b)). This movement allows PEs to maintain more recently used cache lines closer to the Chameleon Virtualizer as shown in Figure 8(c).

The final design consideration of our NUCA C-mode is the placement of the cache control array. In a decoupled design, the cache control array is located in row 0, nearest to the Chameleon Virtualizer, reducing the tag look-up latency significantly. Our NUCA design adopts a decoupled design as its base so that the Chameleon Virtualizer can detect the location of the target data line early in its look-up stage. By moving the cache control bits across PEs in row 0, as shown in Figure 8(d), we can force the y -coordinate of a PE that keeps the target data line to be always bigger by one than the x -coordinate of a PE that keeps the target control bits. For example, if the x -coordinate of the PE that has the control bits of the requested cache line is 3, the Chameleon Virtualizer can find corresponding data line in row 4.

Furthermore, we added another special move instruction to optimize the access latency of NUCA designs. This instruction is executed by PEs in row 1 but ignored by PEs in other rows. Upon decoding this instruction, the PEs

in row 1 snoop the ORTree bus and store the values of the ORTree into a destination register. With this instruction, the PEs in row 1 can obtain the hit line directly when the line is transferred to the Chameleon Virtualizer. Without this instruction, the Chameleon Virtualizer has to read back this cache line and write it to the PEs using IBus, which takes at least eight cycles in our baseline architecture.

3.2 P-Mode: Virtualizing Idle Cores as a Prefetcher

In addition to the C-mode that supplies a virtualized last-level cache, we also investigate the enabling mechanisms to reconfiguring idle PEs to work as a data prefetcher. The rationale behind this is from the following observation—the off-chip bandwidth of a heterogeneous multicore processor is typically very large for fulfilling the heavy input demand of the acceleration cores. This bandwidth, when running single-thread applications, may be left unused. Reusing this bandwidth resource to perform data prefetching can potentially improve performance. Even in the scenarios when the prefetches issued are less accurate, they would unlikely affect the overall memory performance if the amount of off-chip bandwidth can satisfy both demand fetches and prefetches. We call this prefetching operation mode of the PE array *P-mode* (or prefetching mode).

In this article, we evaluate two data prefetchers for Chameleon P-mode: a Markov prefetcher [Joseph and Grunwald 1997] and a program counter (PC)-indexed delta correlation prefetcher [Kandiraju and Sivasubramaniam 2002; Nesbit and Smith 2004]. We chose these prefetchers because they use reasonably large prefetch tables to track miss addresses. These are nontrivial overheads to the hardware if implemented exclusively for prefetching purposes. Hence, even state-of-the-art processors do not adopt such implementations, rather, they implemented a simpler next-line prefetcher [Hegde 2008] or a stride prefetcher [Tendler et al. 2001]. We will demonstrate that Chameleon can realize such area-consuming schemes by virtualizing the resources in P-mode.

In the P-mode, the prefetch table is virtually laid out across PEs. Upon an L2 cache miss, the Chameleon Virtualizer checks its prefetch buffer first (Figure 2). If the requested line is not found, then the Chameleon Virtualizer broadcasts microcode to look up the virtualized prefetch table. This microcode drives each PE to perform index hashing, to match tag bits, and to route a target prefetch table entry back to the Chameleon Virtualizer. Then, the Chameleon Virtualizer decodes the table entry and generates prefetch requests. To support P-mode, we added a small data prefetch buffer (a 32-entry buffer in this article) in the Chameleon Virtualizer as shown in Figure 2. A prefetched cache line is temporarily stored in this buffer, which is checked on every L2 cache miss.

3.2.1 Virtualized Markov Prefetcher. Figure 9(a) shows the prefetch table design for a virtualized Markov prefetcher. Although the original Markov prefetcher paper [Joseph and Grunwald 1997] showed that a prefetch table with four next-miss addresses provides a reasonable balance between coverage

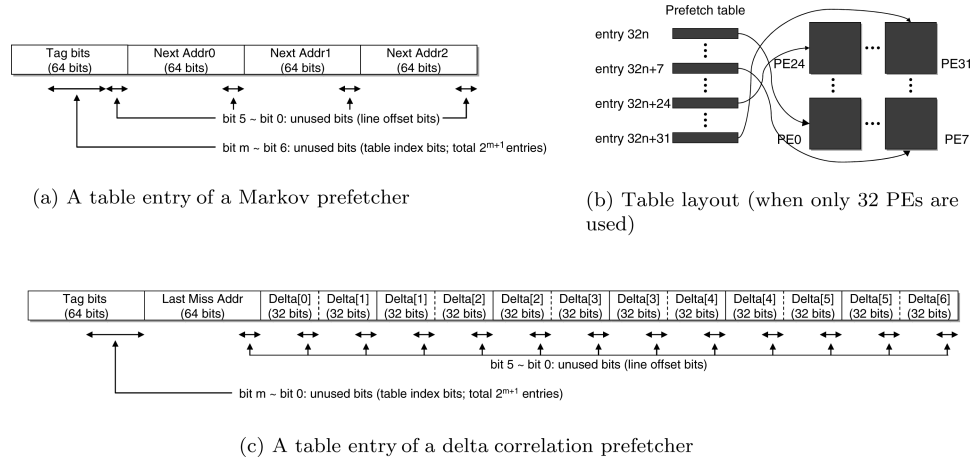


Fig. 9. P-mode prefetcher.

and accuracy, implementing a virtualized Markov prefetcher with four next-miss addresses per entry is challenging because the number of entries per PE should be a power of 2 for simpler PE indexing and because an entry with four next-miss addresses requires at least 40B (larger than 32B but significantly smaller than 64B). In other words, an entry with four next-miss addresses requires 64B with 24B of unused bits, which results in area inefficiency. Thus, we evaluate a Markov prefetcher with three (instead of four) next-miss addresses. As shown in the figure, the size of the prefetch table entry is 32B, and one entry consists of the 8B current-miss address in the tag and three 8B next-miss addresses. Clearly, this design contains unused bits, that is, table index bits and line offset bits (Figure 9(a)), which results in area inefficiency. However, we cannot compact the table entry because a 8B load or a 8B store instruction of a PE is aligned at an 8B boundary. In our proposed design, 4,096 entries can be stored in each PE's local scratchpad memory space.

The P-mode Markov prefetcher is indexed by taking a group of bits (e.g., 17 bits on 32 PEs) from a miss address. These index bits consist of PE ID bits (e.g., 5 LSBs on 32 PEs) and local index bits (e.g., 12 MSBs). The PE ID bits are used to select only one PE that has the target prefetch table entry, while the local index bits are used to generate the memory address of the selected PE's local scratchpad memory. Mapping between the logical table entries and PEs is shown in Figure 9(b). In this example, each prefetch table entry is stored in one of the 32 PEs using the five LSBs of the table index, as shown in the figure. One design issue is the trade-off between the size and latency of the P-mode prefetcher. If there is no need for a large prefetch table, it would be better off to enable only eight PEs in the first row to reduce the look-up latency. In this article, we vary the size of the prefetch table (one, two, four, and eight rows) and perform a sensitivity study in our result section.

The overall procedure is as follows: Upon an L2 cache miss, the Chameleon Virtualizer broadcasts the current data miss address followed by microcode to perform table look-up. This microcode retrieves the hit-prefetch table entry

along with its three next-miss addresses. Then, the Chameleon Virtualizer decodes this return message and generates three prefetch requests.

3.2.2 Virtualized Delta Correlation Prefetcher. In addition to a Markov prefetcher, we also evaluate a delta correlation prefetcher [Kandiraju and Sivasubramaniam 2002; Nesbit and Smith 2004] that keeps the seven latest address delta values. In this delta correlation prefetcher, we compare a pair of two consecutive delta values, (δ_i, δ_{i+1}) ($2 \leq i \leq 5$), with the pair of two latest consecutive delta values, (δ_0, δ_1) , where δ_n is the n^{th} latest delta value. Figure 9(c) shows a prefetch table entry of a P-mode delta correlation prefetcher. The size of each entry is 64B: 8B for tag bits, 8B for the last miss address, and six pairs of 4B delta values. As shown in the figure, instead of keeping seven distinct delta values, our implementation keeps six pairs of two consecutive delta values. In other words, we keep redundant delta values between neighboring pairs. For example, the first pair consists of δ_0 and δ_1 while the second pair consists of δ_1 and δ_2 (Figure 9(c)). Clearly, such data layout is inefficient in terms of area. However, we found that with this layout, we can accelerate the correlation matching process by performing an 8B comparison operation instead of performing two 4B comparison operations or concatenating two delta values. Furthermore, this layout is not perfect in terms of the number of bits due to those unused bits, that is, table index bits and line offset bits (Figure 9(c)). However, due to the same reason as the P-mode Markov prefetcher, the overall table size will be no larger even if we compact the table entry.

As mentioned earlier, the P-mode delta correlation prefetcher is indexed by taking several LSBs from the PC. As in the P-mode Markov prefetcher, these index bits are used to locate a target PE and to locate a target table entry within the selected PE's local scratchpad memory. Upon an L2 miss, the Chameleon Virtualizer broadcasts the instruction's PC followed by the microcode to perform the table look-up. This microcode retrieves a corresponding prefetch table entry from one of the PEs, and the Chameleon Virtualizer calculates the next miss address(es) based on the miss address and the delta values stored in this table entry.

3.3 HybridCP-Mode: Virtualizing Idle Cores for Caching and Prefetching

Instead of dedicating all idle cores as either a last-level cache or a prefetcher, in this section, we propose a hybrid design that virtualize idle cores as a last-level cache backed by a prefetcher. We call this operation mode the *HybridCP-mode*.

Figure 10(a) shows a design of the HybridCP-mode based on a 7MB NUCA WBLP cache and a 128KB prefetch table. As explained earlier, in a NUCA design, 7 PEs in row 0 are filled with cache control bits, while PEs in row 1 to row 7 are filled with cache data. The example shown in the figure places its prefetch table in PE7, which is not utilized in the NUCA WBLP cache. In this example, upon an L2 cache miss, the Chameleon Virtualizer broadcasts cache look-up microcode to all PEs, and it handles returning messages. Once it detects a miss in a virtualized last-level cache, it looks up its prefetch buffer first and broadcasts prefetch table look-up microcode if the target line has not been prefetched. However, because the C-mode microcode and the P-mode microcode

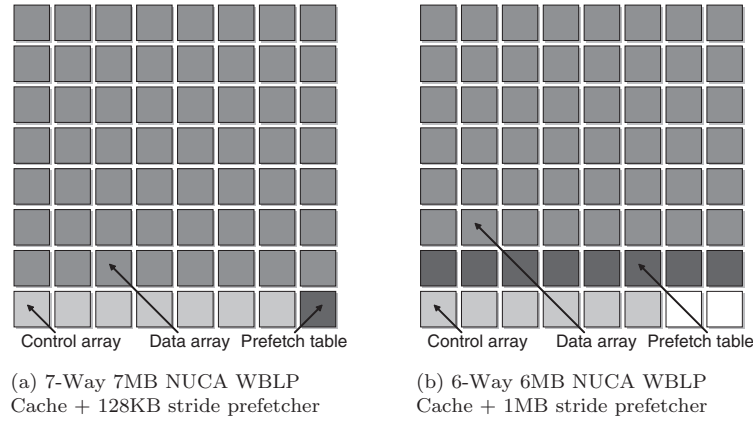


Fig. 10. Hybrid design (cache + prefetcher).

share IBus bandwidth, their operations cannot be overlapped. Figure 10(b) shows another example of the HybridCP-mode in which a 6-way 6MB cache is co-located with a 1MB stride prefetcher table. In this example, the virtualized last-level cache is shrunk, but the prefetch table is enlarged. Note that certain partitioning such as a 4MB cache and a 3MB prefetch table may be infeasible due to PE indexing.

3.4 AdaptiveCP-Mode: Mode Adaptation in Chameleon

Although we have a wide spectrum of Chameleon design space, it is unlikely that any single design choice will prevail in performance for all applications due to the unpredictability of the characteristics in the algorithms and their workloads. A hybrid design will perform better when the host processor runs an application with good locality and a reasonable size of working set. However, when the host processor runs a streaming application (high L3 miss rate), due to its additional cache look-up latency, a hybrid design may perform worse than one with data prefetching capability only. Furthermore, some applications are purely computation-intensive, thus Chameleon will not help to improve the overall performance but consume more power. To obtain the best breed of all, we propose an adaptive mode that dynamically selects one of these Chameleon modes. As Chameleon itself is built on microcode-controlled PEs, an adaptive mode can be implemented at mild hardware cost: Changing the microcode PC to be executed, adding a couple of performance counters, and adding additional control logic in the Chameleon Virtualizer.

Figure 11 shows an example of mode transition for our adaptive mechanism. Once an application is launched, Chameleon is operated in the HybridCP-mode. If the application does not show good locality or has a large working set resulting in a low hit rate, then Chameleon will disable its cache functionality completely and use only its data prefetching functionality. If the application does not have many L2 cache misses (i.e., measured by MPKC, misses per kilo cycles), then Chameleon disables both caching and prefetching to save power. We do not include cache-only mode as the P-mode prefetcher does not harm

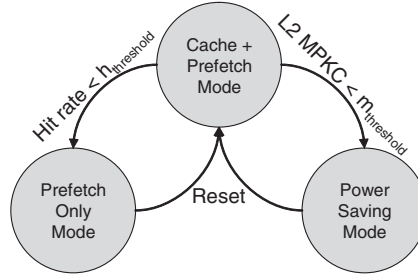


Fig. 11. AdaptiveCP-Mode (MPKC: misses per kilo cycles).

the overall performance, as will be shown in Section 4, because it does not pollute the regular cache hierarchy. To implement an adaptive mechanism, two performance counters are added: an L3 cache hit counter and an L3 cache access counter (equivalent to the L2 cache miss counter). After launching a new process and warming up the C-mode cache, the Chameleon Virtualizer can monitor these two performance counters to make a decision of what mode is more appropriate for the running application. Furthermore, we can perform such sampling regularly by resetting the state diagram to find a better mode when a program phase changes.

4. EXPERIMENTAL RESULTS

4.1 Simulation Environment

Two simulators were used in our analysis. The first one is a cycle-level simulator we developed for the baseline SIMD engine. In addition to an accurate model of PE microarchitecture pipeline, it models latency and bandwidth of the interconnection network among PEs including the IBus, ORTree, MBus, and mesh network. Additionally, we integrated the Chameleon functionality into this simulator. The second simulator is SESC [Renau et al. 2005], a cycle-level architectural simulator. SESC is used to model the host processor, its conventional cache hierarchy, and the off-chip DRAM memory. SESC retrieves latency and throughput³ information measured by the baseline SIMD simulator and uses them to simulate the entire heterogeneous architecture. Table I lists the configuration of the simulated host processor. Unless otherwise stated, the capacity of our baseline L2 cache is 512KB. We also show simulation results with 1MB and 2MB baseline models later. Throughout this article, the baseline performance is measured with this host processor model without any Chameleon capability.

To evaluate the effectiveness of the Chameleon architecture for improving sequential performance, we used the SPEC2006 benchmark suite. The entire SPEC2006 benchmark suite was used except 434.zeusmp, 465.tonto, and 470.lbm, which incurred issues such as cross-compiling failure and unsupported

³In this article, throughput is defined as the number of cycles a cache port is occupied by a cache operation. For example, the throughput of a fully pipelined cache is one, while the throughput of a nonpipelined cache is generally equal to its access latency.

Table I. Host Processor Configuration.

Clock frequency	3.0GHz
Processor model	out-of-order
Machine width	3 (fetch) / 3 (issue) / 3 (retire)
The number of pipeline stages	1 (fetch) / 4 (decode) / 2 (rename) / 4 (wakeup) / 1 (schedule)
ROB size	128
Physical register file size	96 (INT) / 96 (FP)
Branch predictor	Hybrid branch predictor (16K global / local / meta tables), 2K BTB, 32-entry RAS
ITLB	dual-port, 4-way set-associative, 64-entry
DTLB	dual-port, 4-way set-associative, 64-entry
L1 instruction cache	dual-port, 2-way set-associative, 32KB cache with 64B line; 1 cycle hit latency; 1 cycle throughput
L1 data cache	dual-port, 2-way set-associative, 32KB cache with 64B line; 1 cycle hit latency; 1 cycle throughput
L2 cache	single-port, 8-way set-associative, 512KB (1MB, 2MB) cache with 64B line; 15 cycle hit latency; 3 cycle throughput; a stride prefetcher with a 256 entry prefetch table
Memory	Four 64-bit channels, 800MHz double data rate, 350 cycle latency

system calls in our simulators. For all simulations, we fast-forwarded the first 10 billion instructions and simulated next 2 billion instructions.

4.2 Evaluation of C-Mode

First, we measured the latency and throughput for each C-mode design. Unlike a conventional cache where its latency and throughput are solely determined by the characteristics of transistors and wires, the latency and throughput of a C-mode cache are determined by the number of instructions that control PEs and the order of these instructions. For example, for a cache read operation, a read latency can be reduced if instructions that route a read-hit line back to the Chameleon Virtualizer are scheduled earlier than instructions that update LRU bits. On the other hand, the number of the instructions to perform a single cache operation will determine the throughput of a C-mode cache (in a single-bank design) because they consume the IBus bandwidth for the same number of clock cycles. In this work, we wrote microcode using PE assembly code to implement different designs and scheduled them carefully to minimize the latency. The throughput is measured by counting the number of PE instructions to perform a cache operation, and the latency is measured by monitoring the time when a hit/miss signal or a requested cache line is returned to the Chameleon Virtualizer. We assume the PE array operated in the A-mode and C-mode runs at the same frequency of the host processor, 3GHz.

Table II summarizes each cache design and their latency/throughput studied in this section. As shown in Table II, the latency and throughput of NUCA models vary depending on which row an access hits.⁴ Furthermore, even in non-NUCA designs, the throughput can vary depending on whether a hit line

⁴In this article, we use an expression, a hit PE, to address a PE that has a requested cache line in its local scratchpad memory space. Similarly, a hit row is defined as the number of a row to which the hit PE belongs.

Table II. Latency and Throughput of Different C-Mode Designs.

Legend	Description	LRU State of the Hit Line	Read				Write				Replace
			Latency		Throughput		Latency		Throughput		Throughput
			Hit	Miss	Hit	Miss	Hit	Miss	Hit	Miss	
<i>wlp</i>	WLP-style 8-way 4MB	MRU	43	40	44	40	40	40	44	40	37
		non-MRU			46				49		
<i>wblp</i>	WBLP-style 8-way 4MB	MRU	37	36	37	36	36	36	37	36	18
		non-MRU			42				42		
<i>wlp_nuca</i>	Decoupled WLP-style 7-way 7MB	row1 (MRU)	39	21	29	21	20	20	43	20	45
		row2	41		44						
		row3	43		46						
		row4	45		48						
		row5	47		50						
		row6	49		52						
		row7 (LRU)	51		54						
<i>wblp_nuca</i>	Decoupled WBLP-style 7-way 7MB	row1 (MRU)	35	20	24	20	20	20	25	20	23
		row2	37		37						
		row3	39		39						
		row4	41		41						
		row5	43		43						
		row6	45		45						
		row7 (LRU)	47		47						
<i>wlp_8banks</i>	8-bank <i>wlp</i>	Latency and throughput of each bank is same as <i>wlp</i>									

is located at an MRU position or not. When hitting an MRU line, we do not need to update the LRU bits, so the Chameleon Virtualizer does not need to broadcast instructions to update the LRU state.

Not surprisingly, the latency of a WBLP-style cache is lower than that of its WLP-style counterpart. In the case of a WLP-style cache, if the row number of a hit PE is greater than three, the latency of the NUCA design will be worse. In a WBLP-style cache, this threshold will be two. The sophisticated LRU management of NUCA designs is found to be the main reason for this effect.

Table II also shows the read throughput of each design. As shown, there exists a trade-off in throughput between a NUCA design and its counterpart. In the WLP- and WBLP-style caches, not updating the LRU status upon hitting an MRU line helps reduce their throughput by two and five cycles, respectively. A similar trend is observed for the latency and throughput of a write and replacement operation as well.

Now we evaluate and quantify the performance potential for single-thread applications by using the C-mode on a heterogeneous multicore processor. Figure 12 shows the performance impact of different C-mode designs. To show the theoretical limit, we also simulated a perfect memory model in which the L2 cache is assumed perfect. This model also reveals those benchmark programs that are memory intensive. In this article, we define memory-intensive applications as applications whose performance can be improved more than 10% with a perfect L2.

Not surprisingly, the C-mode improves the performance of memory-intensive applications, such as 401.bzip2, 429.mcf, 464.h264ref, 471.omnetpp, 473.as-tar, 483.xalancbmk, 450.soplex, 454.calculix, and 482.sphinx3. For example, the NUCA WBLP-style (*wblp_nuca*) C-mode improves the performance of 483.xalancbmk by 175%. Overall, it is found that the NUCA WBLP-style C-mode is the most effective design. On average (geometric mean), it improves

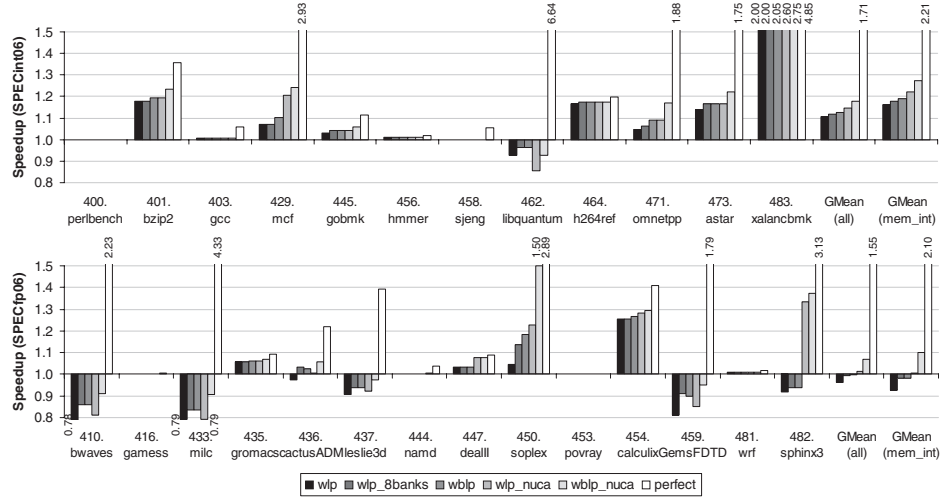


Fig. 12. Relative performance of different C-mode designs.

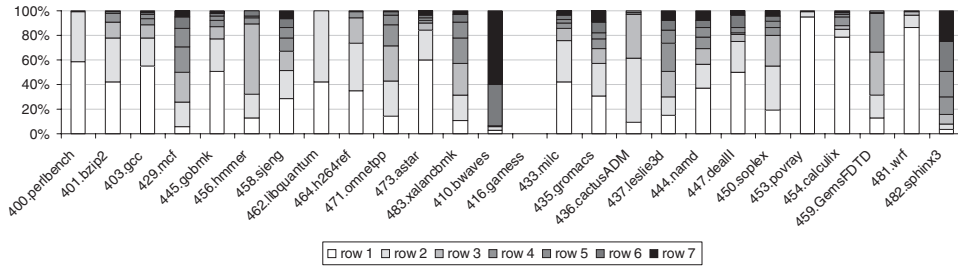


Fig. 13. Distribution of hit rows.

the performance of SPECint06 applications and SPECfp06 by 18% and 7%, respectively. For the memory-intensive application category, the average performance improvements for them are 27% and 10%, respectively.

However, the performance of some memory-intensive applications was degraded including 462.libquantum, 410.bwaves, 433.milc, 437.leslie3d, and 459.GemsFDTD. We found that the hit rates of the C-mode cache were very low when the host processor runs these applications, so an additional cache level will only introduce extra latency in bringing data back.

Apparently, the NUCA models are effective despite their longer latency when a hit PE is located far from the Chameleon Virtualizer. Figure 13 shows the distribution of hit rows. Note that 416.gamess is extremely computation-intensive and generates a small number of cold misses, which results in a 100% L3 miss rate. Therefore, no bar is shown in Figure 13 for it. As shown in Figure 13, most of the cache hits are found in the PEs close to the Chameleon Virtualizer, which justifies the hardware/software effort for addressing the time-zone effect.

Another interesting result is that a multibanked WLP-style cache (*wlp_8banks*) is not as effective as its counterpart: a single-bank WBLP-style cache (*wblp*). As shown in Figure 12, the performance improvement by a

Table III. Latency and Throughput of Different P-Mode Designs.

Legend	Description	Latency	Throughput
Markov1	1MB Markov prefetcher table on 8 PEs in row 0	21	22
Markov2	2MB Markov prefetcher table on 16 PEs in row 0 and 1	23	
Markov4	4MB Markov prefetcher table on 32 PEs in row 0 to 3	27	
Markov8	8MB Markov prefetcher table on 64 PEs in row 0 to 7	35	
delta1	1MB delta correlation prefetcher table on 8 PEs in row 0	37	29
delta2	2MB delta correlation prefetcher table on 16 PEs in row 0 and 1	39	
delta4	4MB delta correlation prefetcher table on 32 PEs in row 0 to 3	43	
delta8	8MB delta correlation prefetcher table on 64 PEs in row 0 to 7	51	

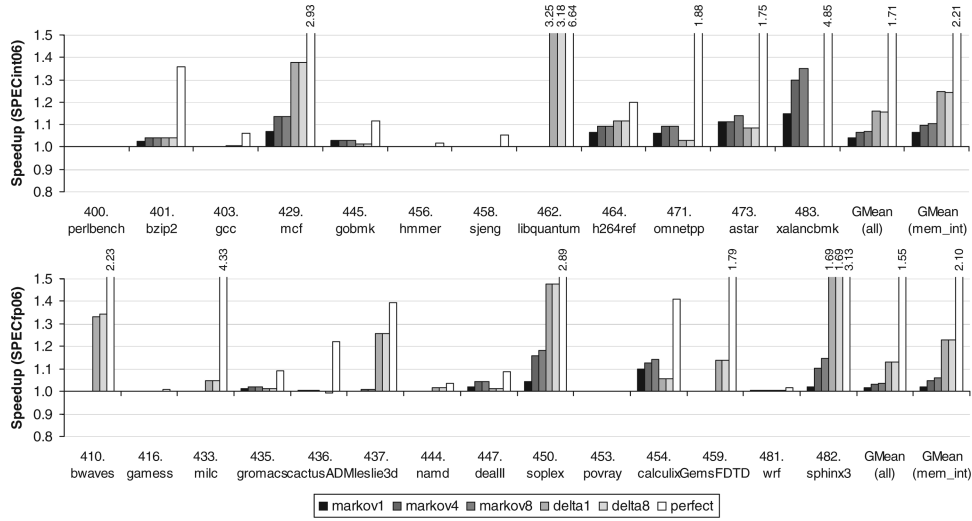


Fig. 14. Relative performance of different P-mode designs.

single-bank WBLP-style cache is always higher than or close to that of its multibanked WLP-style counterpart. This implies that a C-mode cache is accessed infrequently so that designing a faster C-mode cache is more favorable than designing a slower but multibanked C-mode cache.

We also performed simulations with a baseline with a larger L2 cache. On average (geometric mean), when a 1MB L2 cache is used, a NUCA WBLP-style cache improves the performance of SPECint06 and SPECfp06 by 14% and 3%, respectively (21% and 5% for memory-intensive applications). When a 2MB L2 cache is used, the NUCA WBLP-style cache improves the performance of SPECint06 and SPECfp06 by 11% and 2%, respectively (17% and 3% for memory-intensive applications).

4.3 Evaluation of P-Mode

Table III describes each prefetcher design used in this section and shows its table look-up latency and throughput. As expected, we found a trade-off between the table look-up latency and the table size. For example, the look-up latency is 21 cycles for a 1MB Markov prefetcher table while it is 35 cycles for an 8MB table. This trade-off is represented in the overall performance graphs shown in Figure 14. For brevity, we show only the performance result of

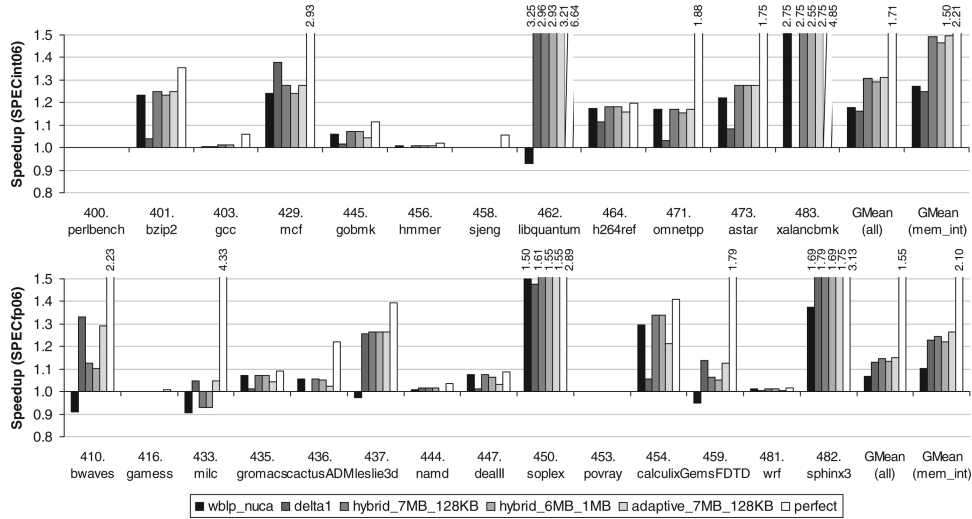


Fig. 15. Relative performance of HybridCP-mode and Adaptivecp-mode.

some prefetcher designs that reveal the trade-off well. For the P-mode Markov prefetcher, a large table is more useful as shown in the simulation results of 483.xalancbmk. This is intuitive because a Markov prefetcher is indexed by a miss address, so a larger table will be able to cover more miss addresses. However, we found that a 1MB P-mode delta correlation prefetcher is sufficiently large because it is indexed by a PC.

In most cases, a P-mode delta correlation prefetcher performs better than a P-mode Markov prefetcher. Seven exceptions are 445.gobmk, 471.omnetpp, 473.astar, 483.xalancbmk, 435.gromacs, 447.deall, and 454.calculix. However, we also found that the performance improvements achieved by a P-mode Markov prefetcher on these applications are actually lower than those by a C-mode cache. In brief, the P-mode Markov prefetcher is less appealing compared to other C-mode caches or the P-mode delta correlation prefetcher. On average, the 1MB P-mode delta correlation prefetcher improved the performance of SPECint06 and SPECfp06 applications by 16% and 13%, respectively. Their average improvements for memory-intensive applications are 25% and 23%.

4.4 Evaluation of HybridCP-Mode and AdaptiveCP-Mode

As shown previously, certain applications benefit more from a C-mode cache while some show more improvement when a P-mode prefetcher is used. For example, the NUCA WBLP-style C-mode cache improves the performance of 483.xalancbmk by 175%, but no improvement is obtained with a 1MB P-mode delta correlation prefetcher. In contrast, the 1MB P-mode delta correlation prefetcher improves the performance of 462.libquantum by 225%, but using the NUCA WBLP-style C-mode cache degrades it by 7%. More interestingly, Figure 15 shows that the HybridCP-mode and the AdaptiveCP-mode can

provide reasonable performance improvement across applications with different characteristics. For easier comparisons, the figure also shows their best performing C-mode (*wblp_nuca*) and P-mode (*delta1*).

Two HybridCP-mode designs were evaluated: a hybrid design with a 7MB NUCA WBLP cache and a 128KB delta correlation prefetcher (*hybrid_7MB_128KB* of Figure 10(a)) and a hybrid design with a 6MB NUCA WBLP cache and a 1MB delta correlation prefetcher (*hybrid_6MB_1MB* of Figure 10(b)). In most cases, the performance difference between these two hybrid designs is small except two applications: 483.xalancbmk and 482.sphinx. As shown in Figure 12, their performance is improved a lot with a bigger cache, and that is why their performance is improved more with the hybrid design with a 7MB NUCA WBLP cache and a 128KB strider prefetcher. On average, this hybrid design improves the performance of SPECint06 and SPECfp06 by 31% and 15%. The average performance improvements for memory-intensive ones are 49% and 24%. (For the remainder of the article, the HybridCP-mode refers to the hybrid design with a 7MB cache and 128KB prefetcher unless explicitly stated otherwise.)

On the other hand, we found an AdaptiveCP-mode can perform as well as the HybridCP-mode. This adaptive one is based on the previous HybridCP-mode with a 7MB NUCA WBLP cache and a 128KB stride prefetcher. However, we disable its cache functionality to behave as a 128KB delta correlation prefetcher based on the algorithm shown in Figure 11. In this evaluation, we modeled the AdaptiveCP-mode to make decisions after warming up the cache during the first 30 million cycles (0.1 ms) and then monitoring the number of cache accesses and hits for the next 30 million cycles. In this set of simulations, we perform this sampling every 600 million cycles (2ms) to find a better Chameleon mode just in case a program phase changes. The model in Figure 15 uses 30% for the threshold of the cache hit rate and 0.5 for the number of L2 misses (= L3 accesses) per kilo cycles (MPKC), which are found to provide the highest average improvement (although not significantly) according to our sensitivity study. As shown in the figure, the AdaptiveCP-mode performs at least as well as the HybridCP-mode. In particular, it prevails when the host processor runs applications favoring a prefetcher, for example, 462.libquantum and 433.milc. On average, the AdaptiveCP-mode improves the performance of SPECint06 and SPECfp06 by 31% and 15%, respectively. For memory-intensive applications, it improves by 50% and 26%, on average. Furthermore, this adaptive design does not degrade the performance of any application. (Note that the only application whose performance is degraded by the HybridCP-mode is 433.milc with a 7% degradation.)

We also performed a sensitivity study with different L2 sizes and summarize their average performance improvements as follows. Using a 1MB L2 cache baseline, the AdaptiveCP-mode improved the performance of SPECint06 and SPECfp06 by 27% and 12%, respectively (43% and 23% for memory-intensive applications). When increasing the capacity to 2MB, it improved the performance of them by 25% and 11%, respectively (40% and 21% for memory-intensive applications).

4.5 Hardware and Power Overhead

The hardware overhead to support Chameleon is insignificant. First of all, the Chameleon Virtualizer requires a prefetch buffer, an MSHR, a Chameleon microcode memory, and corresponding control logic changes. In our simulations, we modeled a 32-entry prefetch buffer and an 8-entry MSHR. In case of the HybridCP-mode, for example, less than 128 PE instructions are required. Thus, a 128-entry Chameleon microcode memory is sufficient to implement both the cache and the prefetcher. Conservatively assuming that supplementary control logic requires the same amount of space of these memory components, the area overhead compared to a baseline SIMD engine is estimated to be 0.01%. In this estimation, we used Intel's data [Hamzaoglu et al. 2008] and Penryn die to estimate the sizes of the Chameleon Virtualizer and the baseline SIMD engine. Second, to support Chameleon, we added two new special “move” instructions explained in Sections 3.1 and 3.1.4. Third, to provide a NUCA model, we added two sets of mux and demux, as shown in Figure 7(b), as well as additional pipeline registers to solve the time-zone effect of the northbound transfer instruction. Fourth, to widen the datapath in a WBLP-style cache, we directly connected IBus and ORTree to the Chameleon Virtualizer without using conventional fan-out and fan-in trees. Note that this new wiring does not require any wiring change in each PE. Lastly, to support the AdaptiveCP-mode, we need to add two performance counters that count the number of accesses and the number of hits in the Chameleon cache.

We also evaluated the extra dynamic power dissipation for the AdaptiveCP-mode using Wattch [Brooks et al. 2000] model. We additionally modeled the global interconnect (IBus, ORTree, Mesh) power consumption using the Berkeley Predictive Technology Model [Cao et al. 2000]. We conservatively modeled the power by assuming the worst-case power consumption in the cache and prefetch operations. For example, if a cache read hits in row 0 of the NUCA model, no data and cache control array migration is required. However, for convenience, we conservatively modeled that all 56 PEs are active regardless of the LRU state of a hit line.

Figure 16 shows the relative power consumption and *performance per joule* of the Adaptive-CP mode. Note that the performance improvement is also shown for easier reference. Although Chameleon consumes a considerable amount of energy by running microcode on 64 PEs, because Chameleon is accessed very infrequently (on an L2 miss), Chameleon will consume only 69% (SPECint06) and 37% (SPECfp06) more power (Figure 16) than the baseline host processor with a conventional L1 and L2 caches. Note that the baseline SIMD engine is already designed to accommodate the power consumption of 64 active PEs. Thus, the power consumption of the AdaptiveCP-mode is still below the total chip power budget. This indicates that Chameleon is more power-efficient than other thread-level speculation techniques for improving sequential performance [Agarwal et al. 2007; Liu et al. 2006]. Although power overhead analysis was not reported in these prior works, their power overhead is likely to exceed the power overhead of Chameleon due to their full utilization of all high-performance cores while Chameleon is only accessed upon an L2 cache miss.

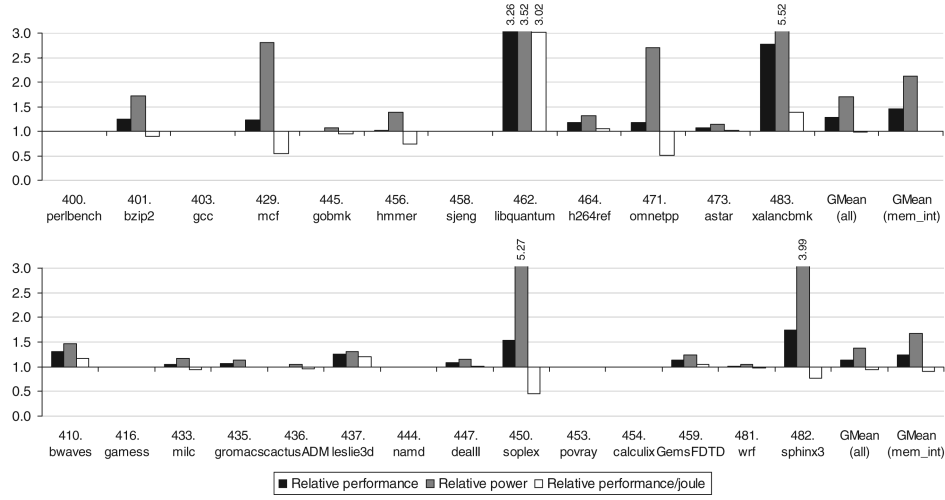


Fig. 16. Performance, power, and performance per joule of the AdaptiveCP-mode.

Figure 16 also shows the energy efficiency represented in performance per joule, which represents achievable speed-up under the same energy budget or energy efficiency. Overall, the AdaptiveCP-mode degrades the performance per joule of SPECint06 and SPECfp06 by 2% and 5% (0.98x and 0.95x in the geomeans). Interestingly, there are some applications whose performance per joule is improved a lot, such as 462.libquantum, 483.xalancbmk, and 437.leslie3d. In other words, as their performance is improved a lot, their energy efficiency can be improved in spite of Chameleon’s power overhead. Another interesting observation is that if the application does not get any benefits using Chameleon, their energy efficiency is not affected as well for Chameleon is rarely accessed. However, energy efficiency of some applications, such as 429.mcf, 456.hmmer, 471.omnetpp, 450.soplex, and 482.sphinx3, is degraded, as shown in Figure 16. We found that they prefer the HybridCP-mode, so they consume much energy upon an L2 cache miss. If one is particularly interested in energy efficiency rather than the performance itself, she or he can tune the threshold values of the adaptive Chameleon so that Chameleon is not turned on when the host processor runs other applications. However, optimizing for energy efficiency is out of scope of this article, and it remains as our future work.

5. IMPLICATIONS TO THE OVERALL DESIGN

In this section, we discuss several issues of Chameleon that are not discussed in the main text, but necessary for completeness.

Context switching. The C-mode cache evaluated in this article is based on a write-through policy. By using a write-through policy, we can avoid the overhead of context switching, a massive data movement from scratchpad memories to the main memory when a newly scheduled data-parallel application wants to use scratchpad memories. Because ample memory bandwidth is left unused due to idleness of acceleration cores, one traditional disadvantage

of a write-through policy, consuming more bus bandwidth, is not critical in the Chameleon architecture. All our simulation results account for all write-through traffic.

Coherence support. Although it is not completely evaluated in this article, cache coherence can be supported by the Chameleon Virtualizer. Upon receiving a coherence message, the Chameleon Virtualizer broadcasts microcode to look up coherence bits stored in one of the PEs (PEs in row 0 in the NUCA design). A state machine needs to be implemented in the Chameleon Virtualizer so that it can perform a correct coherence action upon receiving coherence bits from a PE.

Usage model. Although the baseline PE array is typically used as an accelerator for data-parallel applications, Chameleon enhances it so that it can work better than a conventional superscalar processor, especially for memory intensive applications. If Chameleon is used in an accelerator board on a system bus, for example, PCIe, or integrated onto a CPU chip, a smart OS can schedule memory-intensive workloads on Chameleon rather than on a conventional CPU if it fails to find a data-parallel application. Moreover, Chameleon can enhance the performance of data-parallel applications as well because it improves the performance of their sequential portion of the code.

Dynamic voltage and frequency scaling. Instead of using Chameleon, while PEs are idle, the host processor can exploit remaining power budget by dynamically increasing its clock frequency and supply voltage [Kim et al. 2008; Kumar and Hinton 2009]. Because idle PEs consume a small amount of idle power, the host processor can run at a higher clock frequency without exceeding the overall power budget of the chip. Nonetheless, this method will not be able to improve the performance of memory-intensive, single-thread applications, which are typically unscalable and insensitive to the clock frequency. Chameleon provides an attractive alternative to improve the single-thread performance of memory-intensive applications, as shown in previous sections.

Extension to other architecture. Although we used a heterogeneous multicore processor integrated with an acceleration PE array to demonstrate our techniques, the general idea of virtualizing idle cores is not limited to such platforms but applicable to other similar types of multicore or many-core architectures. Although it is impossible to address all different architecture-specific design issues in a single article, here we briefly describe how our idea can be applied to other architectures. For example, to provide a virtualized last-level cache in the IBM Cell/BE, an interface similar to the Chameleon Virtualizer can be implemented between a power processing element (PPE) and synergetic processing elements (SPEs), forwarding L2 miss traffic to the SPEs instead of sending it directly to the off-chip DRAMs. The new interface may need to broadcast only an L2 miss address along with a small amount of control signals, since IBM Cell SPEs store their code internally. Depending on the look-up outcome, the new interface can route the return message either to the PPE L2 or to the main memory. As Cell SPEs can be used for MIMD processing, they are more suitable to have a highly concurrent multibanked cache than SIMD PEs. The current capacity of the Cell PPE's L2 is 512KB while the aggregate capacity of all local stores of eight SPEs is 2MB. When the number of SPEs scales in the future, the aggregate capacity of local stores will be proportionally larger,

making Chameleon on the future Cell processors more attractive. Another potential platform to apply Chameleon is on-chip integrated GPUs. An interface similar to the Chameleon Virtualizer can be added between an L2 cache and the integrated GPU, and it can forward an L2 miss address to the GPU. Although a GPU does not have much cache or scratchpad memory space, it has very large register files to enable massive multithreading for hiding a cache miss latency. Thus, instead of relying on a scratchpad memory space, we can record prefetch history in the register file of the GPU. This usage model has been demonstrated in a recent article [Woo and Lee 2010].

6. RELATED WORK

Prior studies investigated speculative multithreading or helper thread type of techniques [Sohi et al. 1995; Hammond et al. 1998; Dundas and Mudge 1997; Collins et al. 2001; Luk 2001; Annavaram et al. 2001; Liao et al. 2002; Mutlu et al. 2003] to boost single-thread performance by utilizing idle cores. However, these techniques require acceleration cores to be completely redesigned to support them, which could lead to severe performance degradation when running conventional data-parallel applications. An event-driven helper thread emulates the behavior of a hardware prefetcher on a closely coupled homogeneous idle core [Ganusov and Burtscher 2006]. Others implemented a technique that exploits remaining power budget by scaling the clock frequency and the supply voltage of an active core while the other cores are idle [Kim et al. 2008; Kumar and Hinton 2009].

On the other hand, Cong et al. [2007] proposed core spilling when resources on one core are exhausted. Similarly, Core Fusion [Ipek et al. 2007] was proposed to group independent cores to form a larger CPU dynamically as needed by applications. A flexible heterogeneous multicore processor [Pericas et al. 2007] dynamically adds or removes a processor from the system to adapt to the requirement of the applications.

Software caching techniques have been used by many systems. To improve the programmability of SPEs on IBM Cell/BE, IBM provided a software cache library as a part of their SDK [Arevalo et al. 2008; Eichenberger et al. 2005]. The MIT Raw processor used software caching to emulate both instruction [Miller and Agarwal 2006] and data cache [Moritz et al. 1999], while the Stanford VMP multiprocessor handled cache misses using software techniques [Cheriton et al. 1986]. Furthermore, with advanced compiler techniques, a software cache memory can be better managed [Udayakumaran et al. 2006; Kandemir et al. 2001; Chen et al. 2008]. The goal of all these prior works is to improve the programmability or performance of a processor with local scratchpad memory, while the goal of our work is to provide a virtualized last-level cache to the host processor to improve single-thread performance of the host processor. On the other hand, several studies proposed a reconfigurable memory architecture that can be configured to behave either as a cache memory or as a scratchpad memory [Mai et al. 2000; Sankaralingam et al. 2003; Firoozshahian et al. 2009]. These memory architectures require both a data and a tag array to function as a cache memory.

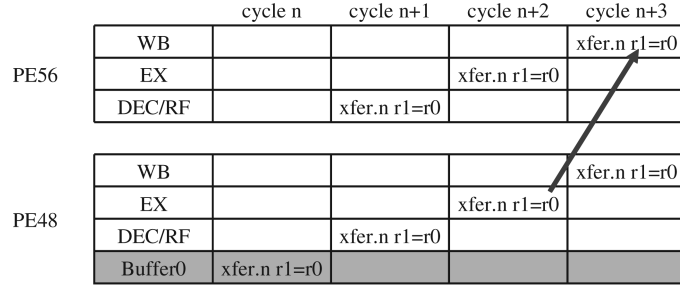
To use on-chip memory resources more efficiently, researchers have focused on managing shared cache memories [Kim et al. 2004; Zhang and Asanovic 2005; Chang and Sohi 2006; Harris 2005; Hsu et al. 2006; Qureshi and Patt 2006; Guo et al. 2007]. Zhang and Asanovic [2005] proposed a new cache management policy called victim replication, which combines the advantage of private and shared schemes in a tiled CMP. Chang and Sohi [2006] used private cache memories for both dynamic sharing and performance isolation. Harris [2005] proposed a synergistic caching policy, which groups neighboring cores into a cluster to have shared memory space among them. These prior studies try to address the problems of shared cache management while our work tries to address the underutilization issue of a heterogeneous multicore processors by virtualizing the unused PEs.

On the other hand, a NUCA cache structure has been studied to tackle a long latency problem of the last-level cache. Kim et al. [2002] proposed an adaptive, nonuniform cache structure. Based on a NUCA model, Huh et al. [2005] studied an optimal degree of cache sharing. Unlike the original NUCA proposal, NuRAPID decouples tag and data array to enable flexible data placement [Chishti et al. 2003]. Although this article adopts an idea of a NUCA cache, we propose an architectural solution called *time-zoning* to provide nonuniform cache access latencies on a SIMD PE engine that has a strictly synchronized execution model.

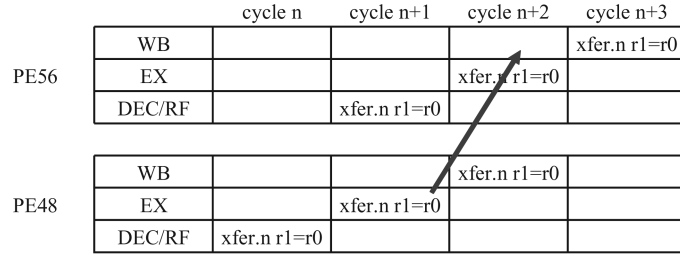
Memory-Mapped I/O (MMIO) is a well-known technique that allows a CPU to assign a part of its memory space to an I/O device and maps it to the memory space of the I/O device. MMIO is mainly used for communication between CPU and I/O devices. The PPE of IBM Cell/BE also has limited capability of accessing the memory space mapped to the local store of SPEs through its MMIO interface, but this is far less efficient than using DMA, and this operation is not synchronized with SPE execution [Kistler et al. 2006]. Chameleon is completely different from MMIO. Chameleon is targeted to improve the performance of the host processor by virtualizing idle cores collectively into a cache and/or a prefetcher. There is no static address mapping involved in Chameleon.

7. CONCLUSION

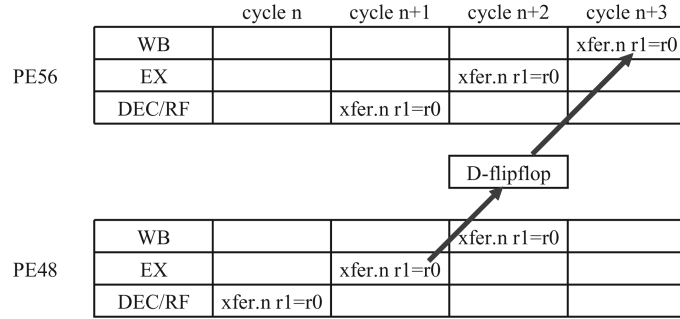
In this article, we propose Chameleon, a flexible heterogeneous multicore processor that virtualizes idle acceleration cores for improving the memory performance of sequential code. To address the underutilization issue when these cores are not used for DLP processing, Chameleon can virtualize these idle cores collectively into a last-level cache (C-mode) or a table-based data prefetcher (P-mode) for single-thread applications running on the host processor. We studied the trade-off between performance and architectural complexity of several caching designs. For data prefetching, we demonstrated the mechanisms to reconfiguring these acceleration cores into a Markov prefetcher and a delta correlation prefetcher. Moreover, we introduce a hybrid mode to enable caching and data prefetching simultaneously using the collective acceleration cores. To achieve the highest efficiency for performance versus energy, we devise an



(a) Conventional, strictly synchronized execution model



(b) Time-Zone effect of the pipelined execution model



(c) Solution for the pipelined execution model

Fig. 17. Conventional and NUCA execution model of `xfer.n` instruction.

adaptive mode to migrate the functionality of Chameleon between the hybrid mode and prefetch-only mode by monitoring the cache behavior.

We used a heterogeneous multicore processor that consists of one high-performance processor core and an array of SIMD-capable processing elements for the case study to demonstrate our techniques in this article. Using the SPEC2006 benchmark suite, we found that, on average, the Chameleon C-mode can improve the performance of SPECint06 and SPECfp06 by 18% and 7% while the Chameleon P-mode can improve them by 16% and 13%. Furthermore, our hybrid mode shows a 31% and 15% improvement, respectively. In the

	cycle n	cycle n+1	cycle n+2	cycle n+3
PE56	WB			xfer.s r1=r0
	EX		xfer.s r1=r0	
	DEC/RF	xfer.s r1=r0		
PE48	WB			xfer.s r1=r0
	EX		xfer.s r1=r0	
	DEC/RF	xfer.s r1=r0		
	Buffer0	xfer.s r1=r0		

(a) Conventional, strictly synchronized execution model

	cycle n	cycle n+1	cycle n+2	cycle n+3
PE56	WB			xfer.s r1=r0
	EX		xfer.s r1=r0	
	DEC/RF	xfer.s r1=r0		
PE48	WB		xfer.s r1=r0	
	EX	xfer.s r1=r0		
	DEC/RF	xfer.s r1=r0		

(b) Time-Zone effect of the pipelined execution model

	cycle n	cycle n+1	cycle n+2	cycle n+3
PE56	WB			
	EX		xfer.s r1=r0	xfer.s r1=r0
	DEC/RF	xfer.s r1=r0		
PE48	WB			xfer.s r1=r0
	EX	xfer.s r1=r0	xfer.s r1=r0	
	DEC/RF	xfer.s r1=r0		

(c) Solution for the pipelined execution model

Fig. 18. Conventional and NUCA execution model of xfer.s instruction.

adaptive mode, 31% and 15% are observed for SPECint06 and SPECfp06. Finally, when accounting for memory-intensive applications only from the suite, the average speed-ups of the adaptive mode are 50% and 26% for SPECint06 and SPECfp06, respectively.

APPENDIX

A. TIME-ZONE EFFECT

In this appendix, we explain the time-zone effect (mentioned in Section 3.1.4) in detail. Unlike the strictly synchronized execution model of the baseline architecture, to support the NUCA model, the instruction and flag queues, originally

designed for synchronizing their broadcasting, are bypassed. In this execution model, different PEs in different rows execute different instructions at the same cycle. However, such a pipelined execution model could complicate the synchronization of the ORTree values and that of northbound and southbound transfer instructions, which we call *time-zone effect*.

Fortunately, the ORTree time-zone effect is not an issue in the C-mode because C-mode microcode uses the ORTree to obtain a requested cache line. Furthermore, the Chameleon Virtualizer is allowed to issue one memory look-up microcode at a time, so there is no concern of data corruption between distinct memory accesses.

The next problem is synchronizing the northbound transfer instruction. This problem is depicted in Figure 17 in which processor pipeline stages of two PEs are shown. Note that Buffer0 stage of PE48 is a pipeline stage introduced by the one-entry instruction queue of PE48. The *xfer.n* instruction is a special type of *move* instruction that copies a register value of a PE into a register of its northern neighbor PE. In synchronized execution (Figure 17(a)), the r0 value of PE48 reaches PE56 at cycle $n + 3$ when the *xfer.n* instruction being executed by PE56 is in the write-back (WB) stage. In this example, PE56 expects to have its r1 value from PE48 as the same *xfer.n* instruction is decoded and being executed by PE56 itself. Therefore, PE56 will set up control signals prior to the reception of the value. However, in the pipelined execution model (Figure 17(b)), the r0 reaches PE56 at cycle $n + 2$ when the same *xfer.n* instruction is in the EX stage. In other words, PE56 has not set up control signals to read the transferred value from PE48, and to update its r1. Without any support, the r1 of PE56 will not be correctly updated. To address this issue, we propose virtually synchronizing this *xfer.n* instruction by adding one more pipeline register in the northbound output mesh driver of PE48, so that the r0 value can reach PE56 at cycle $n + 3$ (Figure 17(c)).

A similar problem is present in synchronizing the southbound transfer *xfer.s* instruction. Figure 18(a) shows the synchronized execution model. However, in the pipelined execution model (Figure 18(b)), the r0 of PE56 reaches PE48 at cycle $n + 3$. At this moment, the *xfer.s* is no longer in the pipeline of PE48. As such, the r1 of PE48 will not be correctly updated. Fortunately, as shown in Figure 18(c), this problem can easily be solved by architecting the latency of this instruction as two cycles. Any instruction that is dependent on the destination register of the *xfer.s* instruction should be scheduled one cycle later, and this is the responsibility of a programmer or a compiler.

REFERENCES

- AGARWAL, M., MALIK, K., WOLEY, K. M., STONE, S. S., AND FRANK, M. I. 2007. Exploiting postdominance for speculative parallelization. In *Proceedings of the 13th International Symposium on High-Performance Computer Architecture*. IEEE, Los Alamitos, CA, 295–305.
- ANNAVARAM, M., PATEL, J. M., AND DAVIDSON, E. S. 2001. Data prefetching by dependence graph precomputation. In *Proceedings of the 28th International Symposium on Computer Architecture*. ACM, New York, 52–61.
- AREVALO, A., MATINATA, R., PANDIAN, M., PERI, E., RUBY, K., THOMAS, F., AND ALMOND, C. 2008. *Programming the Cell Broadband Engine Architecture: Examples and Best Practices*. IBM Redbooks, Armonk, NY.

- ARTIERI, A. 2005. Nomadik: an MPSoC solution for advanced multimedia. In *Proceedings of the 5th International Forum on Application-Specific Multi-Processor SoC*. IEEE, Los Alamitos, CA.
- BROOKS, D., TIWARI, V., AND MARTONOSI, M. 2000. Wattch: A framework for architectural-level power analysis and optimizations. In *Proceedings of the 27th International Symposium on Computer Architecture*. ACM, New York, 83–94.
- BUCK, I. 2007. GPU Computing with NVIDIA CUDA. In *Proceedings of the International Conference on Computer Graphics and Interactive Techniques (SIGGRAPH '07)*. ACM, New York, 6.
- CAO, Y., SATO, T., ORSHANSKY, M., SYLVESTER, D., AND HU, C. 2000. New paradigm of predictive MOSFET and interconnect modeling for early circuit simulation. In *Proceedings of the 2000 Custom Integrated Circuits Conference*. IEEE, Los Alamitos, CA, 201–204.
- CHANG, J. AND SOHI, G. S. 2006. Cooperative caching for chip multiprocessors. In *Proceedings of the 33rd International Symposium on Computer Architecture*. IEEE, Los Alamitos, CA, 264–276.
- CHEN, T., ZHANG, T., SUR, Z., AND TALLADA, M. G. 2008. Prefetching irregular references for software cache on cell. In *Proceedings of the 6th International Symposium on Code Generation and Optimization*. ACM, New York, 155–164.
- CHERITON, D. R., SLAVENBURG, G. A., AND BOYLE, P. D. 1986. Software-controlled caches in the VMP multiprocessor. In *Proceedings of the 13th International Symposium on Computer Architecture*. IEEE, Los Alamitos, CA, 366–374.
- CHISHTI, Z., POWELL, M. D., AND VIJAYKUMAR, T. N. 2003. Distance associativity for high-performance energy-efficient non-uniform cache architectures. In *Proceedings of the 36th International Symposium on Microarchitecture*. IEEE, Los Alamitos, CA, 55.
- COLLINS, J. D., WANG, H., TULLSEN, D. M., HUGHES, C., LEE, Y.-F., LAVERY, D., AND SHEN, J. P. 2001. Speculative precomputation: Long-range prefetching of delinquent loads. In *Proceedings of the 28th International Symposium on Computer Architecture*. ACM, New York, 14–25.
- CONG, J., GUOLING, H., JAGANNATHAN, A., REINMAN, G., AND RUTKOWSKI, K. 2007. Accelerating sequential applications on CMPs using core spilling. *IEEE Trans. Paral. Distrib. Syst.* 18, 8, 1094–1107.
- DALLY, W. J. AND TOWLES, B. 2001. Route packets, not wires: On-chip interconnection networks. In *Proceedings of the 38th Design Automation Conference*. ACM, New York, 684–689.
- DUNDAS, J. AND MUDGE, T. 1997. Improving data cache performance by pre-executing instructions under a cache miss. In *Proceedings of the 11th International Conference on Supercomputing*. ACM, New York, 68–75.
- DUTTA, S., JENSEN, R., AND RIECKMANN, A. 2001. Viper: a multiprocessor SOC for advanced set-top box and digital TV systems. *IEEE Des. Test Comput.* 18, 5, 21–31.
- EICHENBERGER, A. E., O'BRIEN, K., O'BRIEN, K., WU, P., CHEN, T., ODEN, P. H., PRENER, D. A., SHEPHERD, J. C., SO, B., ET AL. 2005. Optimizing compiler for the CELL processor. In *Proceedings of the 14th International Conference on Parallel Architectures and Compilation Techniques*. IEEE, Los Alamitos, CA, 161–172.
- FIROOZSHAHIAN, A., SOLOMATNIKOV, A., SHACHAM, O., ASGAR, Z., RICHARDSON, S., KOZYRAKIS, C., AND HOROWITZ, M. 2009. A memory system design framework: creating smart memories. In *Proceedings of the 36th International Symposium on Computer Architecture*. ACM, New York, 406–417.
- GANUSOV, I. AND BURTSCHER, M. 2006. Efficient emulation of hardware prefetchers via event-driven helper threading. In *Proceedings of the 15th International Conference on Parallel Architectures and Compilation Techniques*. ACM, New York, 144–153.
- GHULOUM, A., SMITH, T., WU, G., ZHOU, X., FANG, J., GUO, P., SO, B., RAJAGOPALAN, M., CHEN, Y., ET AL. 2007. Future-proof data parallel algorithms and software on IntelTM multi-core architecture. *Intel Tech. J.* 11, 4.
- GUO, F., SOLIHIN, Y., ZHAO, L., AND IYER, R. 2007. A framework for providing quality of service in chip multi-processors. In *Proceedings of the 40th International Symposium on Microarchitecture*. IEEE, Los Alamitos, CA, 343–355.
- HAMMOND, L., WILLEY, M., AND OLUKOTUN, K. 1998. Data speculation support for a chip multiprocessor. In *Proceedings of the 8th International Conference on Architectural Support for Programming Languages and Operating Systems*. ACM, New York, 58–69.

- HAMZAOGU, F., ZHANG, K., WANG, Y., AHN, H., BHATTACHARYA, U., CHEN, Z., NG, Y., PAVLOV, A., SMITS, K., ET AL. 2008. A 153Mb-SRAM design with dynamic stability enhancement and leakage reduction in 45nm high-K metal-gate CMOS technology. In *Proceedings of the IEEE International Solid-State Circuits Conference*. IEEE, Los Alamitos, CA, 376–621.
- HARRIS, S. 2005. Synergistic caching in single-chip multiprocessors. Ph.D. thesis, Stanford University.
- HEGDE, R. 2008. Optimizing application performance on Intel © Core™ microarchitecture using hardware-implemented prefetchers. Intel Software Network. <http://software.intel.com/en-us/articles/optimizing-application-performance-on-intel-core-microarchitecture-using-hardware-implemented-prefetchers>.
- HENSLEY, J. 2007. AMD CTM overview. In *Proceedings of the International Conference on Computer Graphics and Interactive Techniques (SIGGRAPH'07)*. ACM, New York, 7.
- HILL, M. AND MARTY, M. 2008. Amdahl's law in the multicore era. *Computer* 41, 7, 33–38.
- HSU, L. R., REINHARDT, S. K., IYER, R., AND MAKINENI, S. 2006. Communist, utilitarian, and capitalist cache policies on CMPs: caches as a shared resource. In *Proceedings of the 15th International Conference on Parallel Architectures and Compilation Techniques*. ACM, New York, 13–22.
- HUH, J., KIM, C., SHAFI, H., ZHANG, L., BURGER, D., AND KECKLER, S. W. 2005. A NUCA substrate for flexible CMP cache sharing. In *Proceedings of the 19th International Conference on Supercomputing*. ACM, New York, 31–40.
- IPEK, E., KIRMAN, M., KIRMAN, N., AND MARTINEZ, J. F. 2007. Core fusion: accommodating software diversity in chip multiprocessors. In *Proceedings of the 34th International Symposium on Computer Architecture*. ACM, New York, 186–197.
- JOSEPH, D. AND GRUNWALD, D. 1997. Prefetching using Markov predictors. In *Proceedings of the 24th International Symposium on Computer Architecture*. ACM, New York, 252–263.
- KADOTA, H., MIYAKE, J., OKABAYASHI, I., MAEDA, T., OKAMOTO, T., NAKAJIMA, M., AND KAGAWA, K. 1987. A 32-bit CMOS microprocessor with on-chip cache and TLB. *IEEE J. Solid-State Circuits* 22, 5, 800–807.
- KANDEMIR, M., RAMANUJAM, J., IRWIN, J., VIJAYKRISHNAN, N., KADAYIF, I., AND PARIKH, A. 2001. Dynamic management of scratch-pad memory space. In *Proceedings of the 38th Design Automation Conference*. ACM, New York, 690–695.
- KANDIRAJU, G. B. AND SIVASUBRAMANIAM, A. 2002. Going the distance for TLB prefetching: an application-driven study. In *Proceedings of the 29th International Symposium on Computer Architecture*. IEEE, Los Alamitos, CA, 195–206.
- KIM, C., BURGER, D., AND KECKLER, S. W. 2002. An adaptive, non-uniform cache structure for wire-delay dominated on-chip caches. In *Proceedings of the 10th International Conference on Architectural Support for Programming Languages and Operating Systems*. ACM, New York, 211–222.
- KIM, S., CHANDRA, D., AND SOLIHIN, Y. 2004. Fair cache sharing and partitioning in a chip multiprocessor architecture. In *Proceedings of the 13th International Conference on Parallel Architectures and Compilation Techniques*. IEEE, Los Alamitos, CA, 111–122.
- KIM, W., GUPTA, M., WEI, G., AND BROOKS, D. 2008. System level analysis of fast, per-core DVFS using on-chip switching regulators. In *Proceedings of the 14th International Symposium on High Performance Computer Architecture*. IEEE, Los Alamitos, CA, 123–134.
- KISTLER, M., PERRONE, M., AND PETRINI, F. 2006. Cell multiprocessor communication network: built for speed. *IEEE MICRO* 26, 3, 10–23.
- KUMAR, R. AND HINTON, G. 2009. A family of 45nm IA processors. In *Proceedings of the IEEE International Solid-State Circuits Conference*. IEEE, Los Alamitos, CA, 58–59.
- LIAO, S. S., WANG, P. H., WANG, H., HOFLEHNER, G., LAVERY, D., AND SHEN, J. P. 2002. Post-pass binary adaptation for software-based speculative precomputation. In *Proceedings of the ACM SIGPLAN Conference on Programming Language Design and Implementation*. ACM, New York, 117–128.
- LIU, W., TUCK, J., CEZE, L., AHN, W., STRAUSS, K., RENAULT, J., AND TORRELLAS, J. 2006. POSH: a TLS compiler that exploits program structure. In *Proceedings of the 11th ACM SIGPLAN Symposium on Principles and Practice of Parallel Programming*. ACM, New York, 158–167.

- LUK, C.-K. 2001. Tolerating memory latency through software-controlled pre-execution in simultaneous multithreading processors. In *Proceedings of the 28th International Symposium on Computer Architecture*. ACM, New York, 40–51.
- MAHESRI, A., JOHNSON, D., CRAO, N., AND PATEL, S. J. 2008. Tradeoffs in designing accelerator architectures for visual computing. In *Proceedings of the 41st International Symposium on Microarchitecture*. IEEE, Los Alamitos, CA, 164–175.
- MAI, K., PAASKE, T., JAYASENA, N., HO, R., DALLY, W. J., AND HOROWITZ, M. 2000. Smart memories: a modular reconfigurable architecture. In *Proceedings of the 27th International Symposium on Computer Architecture*. ACM, New York, 161–171.
- MCCOOL, M. D., WADLEIGH, K., HENDERSON, B., AND LIN, H.-Y. 2006. Performance evaluation of GPUs using the RapidMind development platform. In *Proceedings of the ACM/IEEE Conference on Supercomputing*. ACM, New York, 181.
- MILLER, J. E. AND AGARWAL, A. 2006. Software-based instruction caching for embedded processors. In *Proceedings of the 12th International Conference on Architectural Support for Programming Languages and Operating Systems*. ACM, New York, 293–302.
- MOORE, C. 2007. The role of accelerated computing in the multi-core era. In *Proceedings of the Workshop on Manycore and Multicore Computing: Architectures, Applications And Directions*.
- MORITZ, C. A., FRANK, M., LEE, W., AND AMARASINGHE, S. 1999. Hot pages: software caching for raw microprocessors. Tech. rep. MIT-LCS-TM-599, Massachusetts Institute of Technology.
- MUNSHI, A. 2008. OpenCL: parallel computing on the GPU and CPU. In *Proceedings of the International Conference on Computer Graphics and Interactive Techniques (SIGGRAPH '08)*. ACM, New York.
- MUTLU, O., STARK, J., WILKERSON, C., AND PATT, Y. N. 2003. Runahead execution: an alternative to very large instruction windows for out-of-order processors. In *Proceedings of the 9th International Symposium on High-Performance Computer Architecture*. IEEE, Los Alamitos, CA, 129.
- NESBIT, K. AND SMITH, J. 2004. Data cache prefetching using a global history buffer. In *Proceedings of the 10th International Symposium on High Performance Computer Architecture*. IEEE, Los Alamitos, CA, 96–106.
- PAPAKIPOS, M. 2006. PeakStream platform. In *Proceedings of the ACM/IEEE Conference on Supercomputing Tutorial on GPGPU*.
<http://www.gpgpu.org/sc2006/slides/12.papakipos.peakstream.pdf>.
- PERICAS, M., CRISTAL, A., CAZORLA, F. J., GONZALEZ, R., JIMENEZ, D. A., AND VALERO, M. 2007. A flexible heterogeneous multi-core architecture. In *Proceedings of the 16th International Conference on Parallel Architecture and Compilation Techniques*. IEEE, Los Alamitos, CA, 13–24.
- PHAM, D., ASANO, S., BOLLIGER, M., DAY, M. N., HOFSTEE, H. P., JOHNS, C., KAHLE, J., KAMEYAMA, A., KEATY, J., ET AL. 2005. The design and implementation of a first-generation CELL processor. In *Proceedings of the IEEE International Solid-State Circuits Conference*. IEEE, Los Alamitos, CA.
- QURESHI, M. K. AND PATT, Y. N. 2006. Utility-based cache partitioning: a low-overhead, high-performance, runtime mechanism to partition shared caches. In *Proceedings of the 39th International Symposium on Microarchitecture*. IEEE, Los Alamitos, CA, 423–432.
- RENAU, J., FRAGUELA, B., TUCK, J., LIU, W., PRVULOVIC, M., CEZE, L., SARANGI, S., SACK, P., STRAUSS, K., ET AL. 2005. SESC simulator. <http://sesc.sourceforge.net>.
- SANKARALINGAM, K., NAGARAJAN, R., LIU, H., KIM, C., HUH, J., BURGER, D., KECKLER, S. W., AND MOORE, C. R. 2003. Exploiting ILP, TLP, and DLP with the polymorphous TRIPS architecture. In *Proceedings of the 30th International Symposium on Computer Architecture*. ACM, New York, 422–433.
- SIEGEL, H. J., SCHWEDERSKI, T., NATHANIEL J. DAVIS, I., AND KUEHN, J. T. 1984. PASM: a reconfigurable parallel system for image processing. *SIGARCH Comput. Archit. News* 12, 4, 7–19.
- SINGH, H., LEE, M.-H., LU, G., BAGHERZADEH, N., KURDAHI, F. J., AND FILHO, E. M. C. 2000. MorphoSys: an integrated reconfigurable system for data-parallel and computation-intensive applications. *IEEE Trans. Comput.* 49, 5, 465–481.
- SMITH, S. L. 2008. Intel roadmap overview. Intel Developer Forum.
- SOHI, G. S., BREACH, S. E., AND VIJAYKUMAR, T. N. 1995. Multiscalar processors. In *Proceedings of the 22nd International Symposium on Computer Architecture*. ACM, New York, 414–425.

- TENDLER, J., DODSON, S., FIELDS, S., LE, H., AND SINHARROY, B. 2001. POWER4 system microarchitecture. IBM Technical white paper.
- UDAYAKUMARAN, S., DOMINGUEZ, A., AND BARUA, R. 2006. Dynamic allocation for scratch-pad memory using compile-time decisions. *ACM Trans. Embed. Comput. Syst.* 5, 2, 472–511.
- WOO, D. H., FRYMAN, J. B., KNIES, A. D., ENG, M., AND LEE, H.-H. S. 2008. POD: a 3D-integrated broad-purpose acceleration layer. *IEEE Micro* 28, 4, 28–40.
- WOO, D. H. AND LEE, H.-H. S. 2008. Extending Amdahl's law for energy-efficient computing in the many-core era. *IEEE Comput.* 41, 12, 24–31.
- WOO, D. H. AND LEE, H.-H. S. 2010. COMPASS: a programmable data prefetcher using idle GPU shaders. In *Proceedings of the 15th International Conference on Architectural Support for Programming Languages and Operating Systems*. ACM, New York, 297–310.
- YEH, T. Y., FALOUTSOS, P., PATEL, S. J., AND REINMAN, G. 2007. ParallAX: an architecture for real-time physics. In *Proceedings of the 34th International Symposium on Computer Architecture*. ACM, New York, 232–243.
- ZHANG, M. AND ASANOVIC, K. 2005. Victim replication: maximizing capacity while hiding wire delay in tiled chip multiprocessors. In *Proceedings of the 32nd International Symposium on Computer Architecture*. IEEE, Los Alamitos, CA, 336–345.

Received December 2008; revised September 2009; accepted September 2009